

A novel method to sample individual marine snow particles for downstream molecular analyses

Chloé M.J. Baumas ^{1,*} Fatima-Ezzahra Ababou ¹ Marc Garel ^{1,*} Mina Bizic ² Danny Ionescu,² Arthur Puzenat,³ Frederic A.C. Le Moigne ^{1,4} Hans-Peter Grossart,^{2,5} Christian Tamburini ¹

¹Aix-Marseille Université, Université de Toulon, CNRS, IRD, Mediterranean Institute of Oceanography (MIO, UM 110), Marseille, France

²Department of Plankton and Microbial Ecology, Leibniz Institute of Freshwater Ecology and Inland Fisheries (IGB), Stechlin, Germany

³TekCorail, self-employed Arthur Puzenat, Marseille, France

⁴LEMAR Laboratoire des Sciences de l'Environnement Marin, UMR6539, CNRS, UBO, IFREMER, IRD, Technopôle Brest-Iroise, Plouzané, France

⁵Institute of Biochemistry and Biology, Potsdam University, Potsdam, Germany

Abstract

The ocean–atmosphere exchange of carbon largely depends on the balance between carbon export of particulate organic carbon (POC) as sinking marine particles, and POC remineralization by attached microbial communities. Despite the vast spectrum of types, sources, ages, shapes, and composition of individual sinking particles, they are usually considered as a bulk together with their associated microbial communities. This limits our mechanistic understanding of the biological carbon pump (BCP) and its feedback on the global carbon cycle. We established a method to sample individual particles while preserving their shape, structure, and nucleic acids by placing a jellified RNA-fixative at the bottom of drifting sediment traps. Coupling imaging of individual particles with associated 16S rRNA analysis reveals that active bacterial communities are highly heterogeneous from one particle origin to another. In contrast to lab-made particles, we found that complex in situ conditions lead to heterogeneity even within the same particle type. Our new method allows to associate patterns of active prokaryotic and functional diversity to particle features, enabling the detection of potential remineralization niches. This new approach will therefore improve our understanding of the BCP and numerical representation in the context of a rapidly changing ocean.

Oceanic sequestration of carbon dioxide (CO₂) from the atmosphere via the biological carbon pump (BCP) is largely dependent on the formation and sinking of marine particles (Kwon et al. 2009; Siegel et al. 2016, 2023; Le Moigne 2019). These particles often have a high content of organic matter making them hotspots for microbial activity. Particle-attached

*Correspondence: cbaumas@stanford.edu & marc.garel@mio.osupytheas.fr

Author Contribution Statement: C.T. and C.B. conceived the work. C.B. and F.-E.A. developed the RNA-fixative gel recipe. C.B. and F.-E.A. performed the lab experiment with the help of M.G. A.P. sampled plankton by diving. C.B., M.B., and D.I. performed the RNA extraction and amplification of samples from the lab experiment in H.-P.G.'s MIBI lab at IGB. C.B. and M.G. performed the in situ work onboard EMSO-LO cruise. C.B. took the pictures of particles and performed the RNA extraction and amplification of samples from the cruise. M.G. performed the bioinformatic analyses. The writing of the manuscript was led by C.B., F.L.M., and C.T. with significant contribution of all authors.

Additional Supporting Information may be found in the online version of this article.

organisms play a major role in organic matter remineralization and the attenuation of gravitational export fluxes of particulate organic carbon (POC) (Smith et al. 1992; Kjørboe and Jackson 2001; Simon et al. 2002). Sinking particles vary in age and origins (phytoplankton cells, fecal pellets, or aggregated detritus) (Simon et al. 2002; Le Moigne 2019), sinking speeds (Allredge and Silver 1988; Armstrong et al. 2002; Trull et al. 2008; Turner 2015), density, porosity, and fractal dimension (Guidi et al. 2008; Laurenceau-Cornec et al. 2019). Sinking particles constitute unique small ecosystems in continuous interactions with diverse associated microbial communities (Simon et al. 2002; Grossart et al. 2006; Bizic-Ionescu et al. 2018; Baumas and Bizic 2023). In order to predict changes in POC sequestration under future climate scenarios it is crucial to have an exhaustive understanding of the processes attenuating POC fluxes such as microbial degradation. Accordingly, it is essential to provide in situ investigations of the relationship between activity and diversity of particle associated microbial communities with particle type. In the mesopelagic zone (~ 200–1000 m)

where most of the POC flux is attenuated (Martin et al. 1987; Henson et al. 2011; Fuchs et al. 2022), a strong linear relationship was found between prokaryotic heterotrophic production and diversity of active free-living prokaryotes¹ (Baumas et al. 2021). This was, however, not the case for prokaryotes attached to sinking particles.

Microbial communities of individual particles differ largely in activity (Ploug and Grossart 1999; Belcher et al. 2016; Stief et al. 2021), diversity (Thiele et al. 2015; Bizic-Ionescu et al. 2018; Lundgreen et al. 2019; Zäncker et al. 2019) and associated viruses (Szabo et al. 2022). This heterogeneity is partly driven by the history of the particle, and partly by stochastic processes (Cordero and Datta 2016; Bizic-Ionescu et al. 2018). Classifying the type of particles by common characteristics could help revealing some patterns. However, with no operational method to systematically sample individual particles, it remains challenging to include particle heterogeneity into studies on the underlying processes and hence the possibility to discern specific patterns in the activity–diversity relationship.

Studies investigating diversity of particle-attached communities are mostly based on particles collected with a water sampler (such as Niskin bottles or in situ pumps) followed by sequential filtration (e.g., Ganesh et al. 2014; Frank et al. 2016; Salazar et al. 2016; Mestre et al. 2018). However, due to the fragile structure of sinking particles, and their scarcity in the small volumes of sampled water, these methods are inadequate to representatively sample gravitational sinking particles (Allredge and Silver 1988; Planquette and Sherrell 2012; Puigcorb  et al. 2020; Baumas et al. 2021). To target sinking particles and associated microbial communities, alternative approaches such as the marine snow catcher (e.g., Duret et al. 2019; Baumas et al. 2021) or sediment traps (Baumas and Bizic 2023 and references within) have been used. Yet, most of these studies still use a filtration step. This is inadequate for studying microbial community at the individual particle level.

To overcome these limitations, Thiele et al. (2015) deployed drifting sediment traps with viscous formaldehyde-containing gel to intercept intact individual particles to determine the diversity of attached microbial communities by using catalyzed reporter deposition fluorescence in situ hybridization (CARD-FISH). Nowadays, CARD-FISH, though quantitatively relevant, has largely been substituted by semi-quantitative sequence-based approaches. The latter provide in-depth information on diversity, metabolic potential, or activity of the particle-associated communities. In addition, formaldehyde is known to disturb sequencing-based analysis (De Giorgi et al. 1994; Evers et al. 2011). Despite advances in DNA and RNA retrieval from formaldehyde fixed samples (Hykin et al. 2015; Choi et al. 2017), there are still many benefits in

developing a formalin-free method to sample individual particles for sequence-based down-stream approaches.

We developed an RNA-fixative (RNALater-like)-based gel able to be readily placed at the bottom of drifting sediment trap tubes. This RNA-fixative is commonly used (Gray et al. 2013; Fontanez et al. 2015; Pelve et al. 2017) and can be self-manufactured in the lab at low cost. Our method is easy to implement on board of research vessels and allows easy recovery of structurally intact individual particles for combining imaging with RNA or DNA analysis. Here we report results from the process of the method development and its subsequent application during a field-campaign in the Mediterranean Sea.

Material and methods

RNA-fixative gel recipe

To visualize and recover intact individual particles, the gel must be transparent. The gel must also remain soft enough for the particles to sink into, thus properly preserving all particle characteristics and prevent bulk particles accumulation at the bottom of the collecting cup. To jellyfy the hypersaline RNA-fixative (ca. 700 g L⁻¹) we used sodium carboxymethyl cellulose (CMC, ref. 419,338, Sigma-Aldrich) as other agents turned out to be not efficient.

To generate 100 mL of 50% fixative gel, 50 mL of sterile seawater were poured into a 250-mL glass Schott bottle containing 3 g of CMC. The powder was dissolved by stirring and heating (the gel becomes brown if overheated) and by frequent, vigorous handshaking to break lumps and avoid gel coagulation on the stirrer. When almost dissolved, 50 mL of handmade RNA-fixative solution (40 mL 0.5 M ethylenediamine tetraacetic acid (EDTA) [ref. EU0084, Euro-medex], 25 mL 1 M sodium citrate (ref. S-4641, Sigma-Aldrich) and 700 g ammonium sulfate (ref. 21333.365 AnalaR NORMAPUR[®], VWR) in 935 mL MQ water, pH adjusted to 5.2 using 1 M H₂SO₄) were added into the glass bottle, which was removed from the heater while still being shaken. At this step, the gel must be poured immediately into the sediment trap cup. Any remaining lumps disappeared systematically after 24 h by letting the gel cool down to room temperature. A jam-like consistency is suited (Supporting Information Fig. S1). For method development gels containing 0% and 25% RNA-fixative solution were made as well using 100 mL of seawater and 75 mL of seawater plus 25 mL of RNA-fixative solution, respectively. Higher percentages of RNA-fixative were not feasible as gel formation is prevented.

Lab experiments

Four types of particles were used during the lab experiment which was performed in July 2021 (Table 1). For each particle type, a 2-L cylindrical polycarbonate Nalgene[®] bottle was filled with 300 mL of algal or cyanobacterial cultures at the end of the exponential growth phase (*Thalassiosira guillardii*,

¹Despite its evolutionary inaccuracy (Pace 2006), the term prokaryotes is used in this manuscript for conciseness purposes to refer to Bacteria and Archaea together (Doolittle and Zhaxybayeva 2013).

Table 1. Origins of the four different types of particles used in the lab experiment.

Type name in the paper	Strains	Particle generation
Diatoms	<i>Thalassiosira guillardii</i>	Cultures conditions: 14°C, 12 : 12-h light–dark cycle, 120 $\mu\text{mol photons m}^{-2} \text{ s}^{-1}$ irradiance, F/2 medium enriched with vitamins (Guillard 1975; Guillard and Hargraves 1993). Cultures harvested at the late exponential phase.
Trichodesmium	<i>Trichodesmium erythraeum</i> IMS101	Cultures conditions: 27°C, 12 : 12-h light–dark cycle, 120 $\mu\text{mol photons m}^{-2} \text{ s}^{-1}$ irradiance, YBCII medium amended with trace metal solution and vitamins (Chen et al. 1996). Cultures harvested at the late exponential phase.
Crocospaera	<i>Crocospaera watsonii</i> WH8501	Cultures conditions: 27°C, 12 : 12-h light–dark cycle, 120 $\mu\text{mol photons m}^{-2} \text{ s}^{-1}$ irradiance, YBCII medium amended with trace metal solution and vitamins (Chen et al. 1996). Cultures harvested at the late exponential phase.
Zooplankton detritus	Zooplankton detritus	Plankton was sampled in Marseille Bay at 15 m depth using a plankton net (mesh size 200 μm and 30 cm diameter) pulled by a diver equipped with a diving propulsion vehicle. The resulting community was mainly composed of copepods and salps, fed with a mix of all three phytoplankton cultures in an aquarium. Fecal pellets and carcasses were daily collected from the aquarium and stored frozen at -20°C .

Trichodesmium erythraeum IMS101, or *Crocospaera watsonii* WH8501) or with zooplankton detritus. Seawater for the experiment was collected during the PARTY cruise (May 2021, Mediterranean Sea, 42°47', 525°N 0.5°59', 814 E), pre-filtered through GFF filters (ref. 513-5244 Whatman®, VWR) to remove all living zooplankton and natural particles and stored in the dark at 4°C. All bottles were filled to the top (air-bubble free) with seawater and were placed on a roller table in complete darkness for 7 d to allow for particle formation and microbial particle colonization from the surrounding seawater. Although each particle type has been separated into one tank, seawater with the natural free-living prokaryotes had the same origin.

On the day of the experiment, nine particles of each type were collected from the rolling bottles, marking the starting time (T0) of the experiment. Individual particles were separately frozen at -80°C in 2-mL cryotubes. Around 90 particles of each type were used to run the experiment until their collection (Tf) as described below. All leftover particles from the tanks were mixed, filtered on 0.22- μm pore size filter (ref. GPWP04700 Millipor®, Merck, Germany) and frozen at -80°C , serving as bulk control.

Cups containing RNA-fixative gels (with 0, 25, and 50% of RNA-fixative) were placed at the bottom of sediment trap tubes before slowly adding 5 liters of sterile seawater with a peristaltic pump as commonly done for sediment traps (Fig. 1a,b). To limit disturbance of the gel and therefore the dispersion of RNA-fixative, the peristaltic tube was connected to a 10-mL pipette inserted in the space between the cylinder of the sediment trap and the gel cup (Fig. 1b; Supporting Information Fig. S2). The three sediment trap tubes were then

placed in a 300-liter bath pre-adjusted to 17°C. Around 30 particles of each type were dropped into each tube by 2 operators. We visually observed a certain level of particle aggregation while they were sinking before reaching the gel's surface. To mimic real deployment of drifting sediment traps, the tubes were left in the temperature regulated bath for 4 d prior to recovery. During this time, the sediment traps were covered with an aluminum foil to avoid contamination from the lab environment. After 4 d, all tubes were removed from the water bath and the water above the gels was discarded using a peristaltic pump. Individual particles were pipetted out individually from the gel and stored in cryotubes at -80°C (Fig. 1c).

In situ deployment

Natural particles were sampled in situ on board “The N/O Pourquoi Pas?” during the campaign EMSO-LO at the EMSO-LO station (42°48.30N, 0.5°59.93E, February 2022). For logistic reasons, we deployed four sediment traps (four tubes) in a cross-array ensuring a permanently vertical position of the sampling tubes (KC Denmark A.S.), attached for 12 h to the ship's wire-cable (Fig. 1a). We set the sediment trap cross-array with one tube containing 0% RNA-fixative gel, one tube containing 50% RNA-fixative gel, one tube with sterile seawater (Live), and one tube filled with 2 liters of RNA-fixative and 3 liters of sterile seawater (Poisoned), with the latter two serving as bulk controls. The sterile seawater was sampled 3 d before, filtered through 0.22- μm membranes (ref. 512-3331 Sartobran®, VWR) and placed in the fridge to increase its density so it would not escape from the tube while descending through the water column. The sediment trap was deployed at 300 m depth. Considering the short deployment time (12 h),

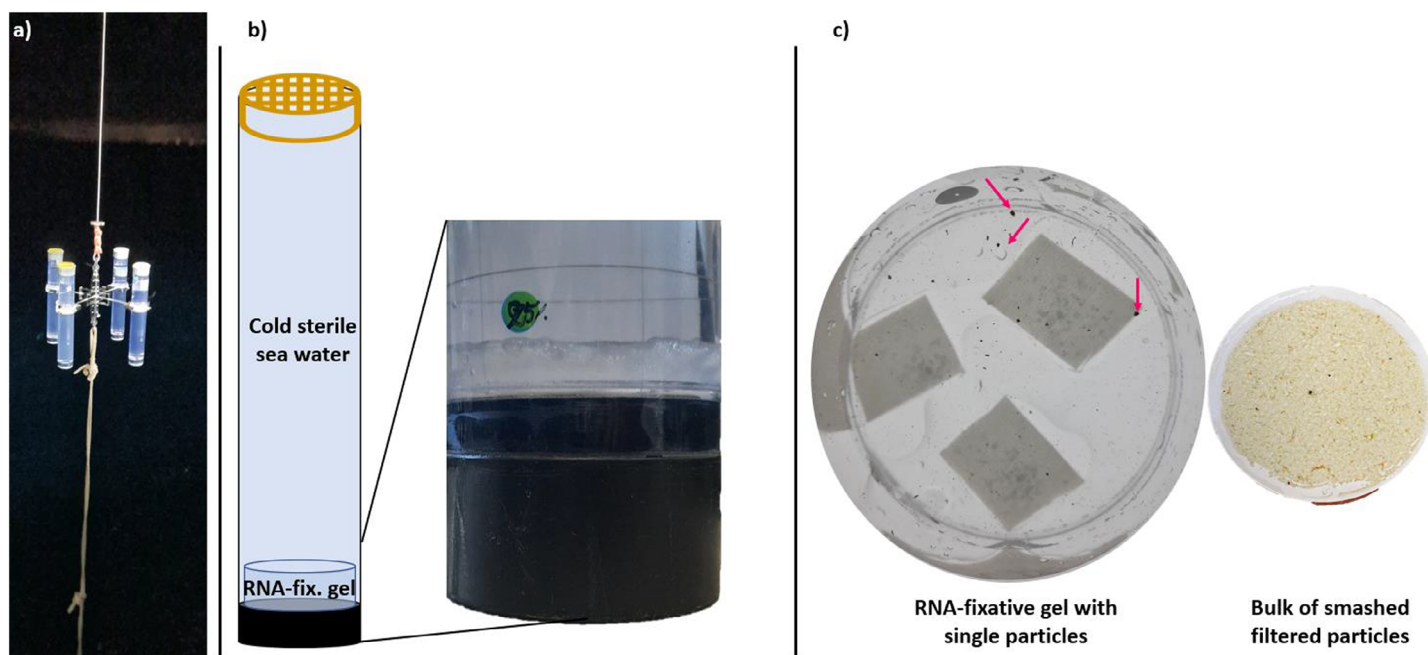


Fig. 1. (a) Picture of the cross-array on which four sediment traps (four tubes) are mounted. (b) Schematic of a sediment trap tube containing a gel cup filled with RNA-fixative gel. The tubes are 700 mm high and 104 mm in diameter. As the cup is 92 mm in diameter, there is space of around 10 mm between tube wall and the cup where a pipette connected to peristaltic pump can be placed to fill the tube without disturbance (see Supporting Information Fig. S2). The associate figure shows a real tube from the lab experiments. (c) Top photographs of individual particles (three examples marked with arrows) whose shapes remained unaffected in the RNA-fixative gels (92 mm in diameter) vs. a bulk filter (45 mm in diameter). The three rectangles at the bottom of the cup are Velcro tabs used to secure the cup to the tube during the deployment.

this depth was chosen as a compromise between strong surface currents that stopped at 225 m, and the relatively low particle concentration at deeper depths.

Recovery of the particles from the gels was done on board using the same procedure as in the lab (see the text above). Cryotubes containing individual particles were stored at -80°C on board the research vessel. In the sediment trap tube containing liquid RNA-fixative, we observed some particles trapped at the interphase between the water and the fixative (due to the density difference), thus the entire 2 liters of fixative were filtered rather than just the bottom. For the sake of comparison, the bulk live sample was treated in the same manner, that is, 3 liters of water from the top of the trap tube were removed and the bottom 2 liters were filtered on 0.22- μm pore size filters (ref. GPWP04700 Millipor[®]) and stored at -80°C (Fig. 1c).

Particle imaging from the EMSO-LO cruise

The RNA-fixative accelerates the formation of salt crystals when defrosted. Therefore, the imaging and subsequent processing have to be done one particle at a time. Cryotubes containing individual particles were removed from -80°C and placed in a benchtop liquid N_2 container. In a sterile area, particles were thawed at room temperature, pipetted carefully using a 1000- μL pipette and placed in individual sterilized small sterile Petri dishes with a high optical transparency

(ref. 10390961, Fisher Scientific). Pictures were then taken using a stereomicroscope (Leica ML165) and the particles were subsequently pipetted into 1.5-mL RNase and DNase-free SafeLock Eppendorf[®] tubes with as little liquid/gel as possible. At this stage, particle structure and shape are no longer important. It is therefore possible to shortly centrifuge the individual samples to remove the leftover gel. To directly proceed with the extraction, 1 μL of RiboLock RNase Inhibitor (ref. EO0381, Thermo Fisher Scientific) and phosphate-buffered saline (ref. 150343, Qiagen) were added to a final volume of 4 μL after which the Eppendorf[®] tube was immersed in liquid N_2 prior to the next steps.

RNA extraction, cDNA synthesis, and metabarcoding library preparation

Individual particles

Following the addition of RiboLock RNase Inhibitor (see section above), cell lysis was performed by four cycles of freeze/thaw, each 1 min in liquid N_2 and 1 min at 65°C . A denaturation step was then performed by adding 3 μL of D2 buffer from the Repli-g single-cell kit (ref. 150343, Qiagen) and incubation for 20 min at 65°C , followed by 3 μL of STOP solution according to the manufacturer's instruction. DNA was digested by adding 1 μL of Turbo DNase ($2 \mu\text{L L}^{-1}$, ref. AM2238 Invitrogen[®], Thermo Fisher Scientific) and incubation for

20 min at 37°C, after which the DNase was deactivated by a 5-min incubation at 85°C.

First-strand cDNA was synthesized with the high-capacity cDNA reverse transcription kit (ref. 4368814 Applied biosystem®, Thermo Fisher Scientific), using 11 µL of template from the previous steps, 1 µL of Multiscribe reverse transcriptase, 2 µL of 10X RT buffer, 0.75 µL of dNTPs, 2 µL of random heptamer primers, and 3.25 µL of H₂O. The 20 µL reverse transcription reaction was set for 10 min at 25°C, 120 min at 37°C, and 5 min at 85°C.

Bulk filters

RNA from bulk filters was extracted as done in Bizic et al. (2022) after which DNA was digested with two steps of 15 min incubation with DNase (1 µL + 1 µL). DNA digestion was verified by negative polymerase chain reaction (PCR) amplification of the remaining RNA, targeting the 16S rRNA gene. First-strand cDNA synthesis was done as above in a 20 µL reaction, however, using 1 µL RNA template.

Library preparations and sequencing

16S rRNA was amplified from the cDNA using the universal primer set targeting Bacteria, 27F (5'-AGRGTTYGATY MTGGCTCAG-3') and 1492R (5'-RGYTACCTTGTACGACTT-3') (Lane 1991; Paliy et al. 2009). The PCR reaction was composed of 3 µL of red reaction buffer (Meridian bioscience-BIO-21109), 1 µL of each primer, 0.75 µL of MyTaq DNA polymerase (5 U µL⁻¹, Meridian bioscience-BIO-21109), 1 µL of MgCl₂ (25 mM, ref. AB0359 Thermo Fisher Scientific), 2 µL of bovine serum albumin (BSA) (20 mg mL⁻¹, ref. 10829410, Fisher Scientific), 10.25 µL of H₂O and 1 µL of cDNA template. The 20 µL reaction was set for 5 min at 95°C, 35 cycles of 45 s at 95°C, 1 s at 52°C, and 1 min at 72°C followed by a final step of 10 min at 72°C. Blank samples were systematically included as control PCR reactions. No nucleic acid from any of our blanks was amplified indicating no detectable contamination during sample processing. Amplicons were then sent to the sequencing facilities at Rush University Genomics and Microbiome Core Facility (Chicago, IL, USA), where the amplification of the V3–V4 regions of the 16S cDNA was performed using the 341F (CCTACGGGNGGCWGCAG) and 785R (GACTACHVGGGTATCTAATCC) primer set (Klindworth et al. 2013). The 16S amplicons were sequenced on a MiSeq platform (Illumina) (paired end 2 × 300 bp). Unfortunately, several sample tubes imploded during air freight resulting in several missing samples. 16S rRNA raw read sequences were deposited to the Short Read Archive under Bioproject number PRJNA934342 (accession number are ranged from SRR23445189 to SRR23445253).

Analysis of sequencing data

The raw sequencing reads were processed using the DADA2 R package (v1.20) (Callahan et al. 2016). The paired-end reads were quality-trimmed (maxEE = c [2,2] for both experiments) and only reads > 200 bp were retained. From a mean of

54,173 ± 18,456 sequences per sample, 60% ± 6% were retained after sequence pre-processing (quality control, merging and chimaera removal). The taxonomic assignment of the amplicon sequence variants (ASVs) was performed using the SILVA_138.1 database (Quast et al. 2013) and functions “assignTaxonomy” and “addSpecies” from the DADA2 R package. Assignment of a sequence to the species level was done only at 100% sequence identity. Both α-diversity and β-diversity were characterized by R packages phyloseq v1.36 (McMurdie and Holmes) and vegan v2.5-7 (Oksanen et al. 2020), after subsampling normalization.

Notation

As the cDNA-based community refers to the actively transcribing microbial community we will refer to these organisms as “active bacteria.”

The term “prokaryotes” refers to Bacteria and Archaea. We use it for the sake of clarity (to refer to both Bacteria and Archaea, Doolittle and Zhaxybayeva 2013) while being aware that it has an inaccurate evolutionary meaning (Pace 2006).

Samples are named according to the following convention L or E for Lab or EMSO-cruise; experimental condition, T0 or percent gel (0, 25, or 50); and particle number. For example, “LT02” refers to the second particle from T0 samples of the lab experiment. T0 bulk, live bulk and poison bulk refer to the mix of particles filtered at T0, or after incubation in the sediment trap.

Results

Gel recipe

RNA-fixative is challenging to jellify due to its salt supersaturation (around 700 g L⁻¹). Of the differently tested protocols only the use of CMC (sodium carboxymethyl cellulose, Sigma-Aldrich, ref. 419338; see “Materials and Methods” section) resulted in adequate fixative gel properties. Alternative combinations of powders (e.g., gelatin powder, Sephadex, agar, agarose, acrylamide, magnesium sulfate powder, ammonium persulfate (APS) powder) and protocols (heated or not, different proportions of powder, different proportion of the RNA-fixative or mix between reagents) led to either over liquefied, over crystallized or opaque products.

Based on visual inspection, we concluded that covering gels tightly with parafilm, allows storage for at least 3 months at 4°C and 2 months at room temperature, allowing to easily generate and transport the gels before campaigns (even a few months in advance as is the case of container shipping). Particle structure, shape, and size remain unchanged after freezing at –80°C and thawing at ambient temperature, demonstrating the ability to freeze the samples until the final analyses.

Comparison of colonizers of lab-made particles

The number of active bacterial ASVs varied with particle type, with a mean of 103 ± 13, 85 ± 12, 48 ± 10, and 224 ± 99 ASVs for *Crocospaera*, Diatoms, *Trichodesmium*, and zooplankton detritus, respectively. Some bacterial families

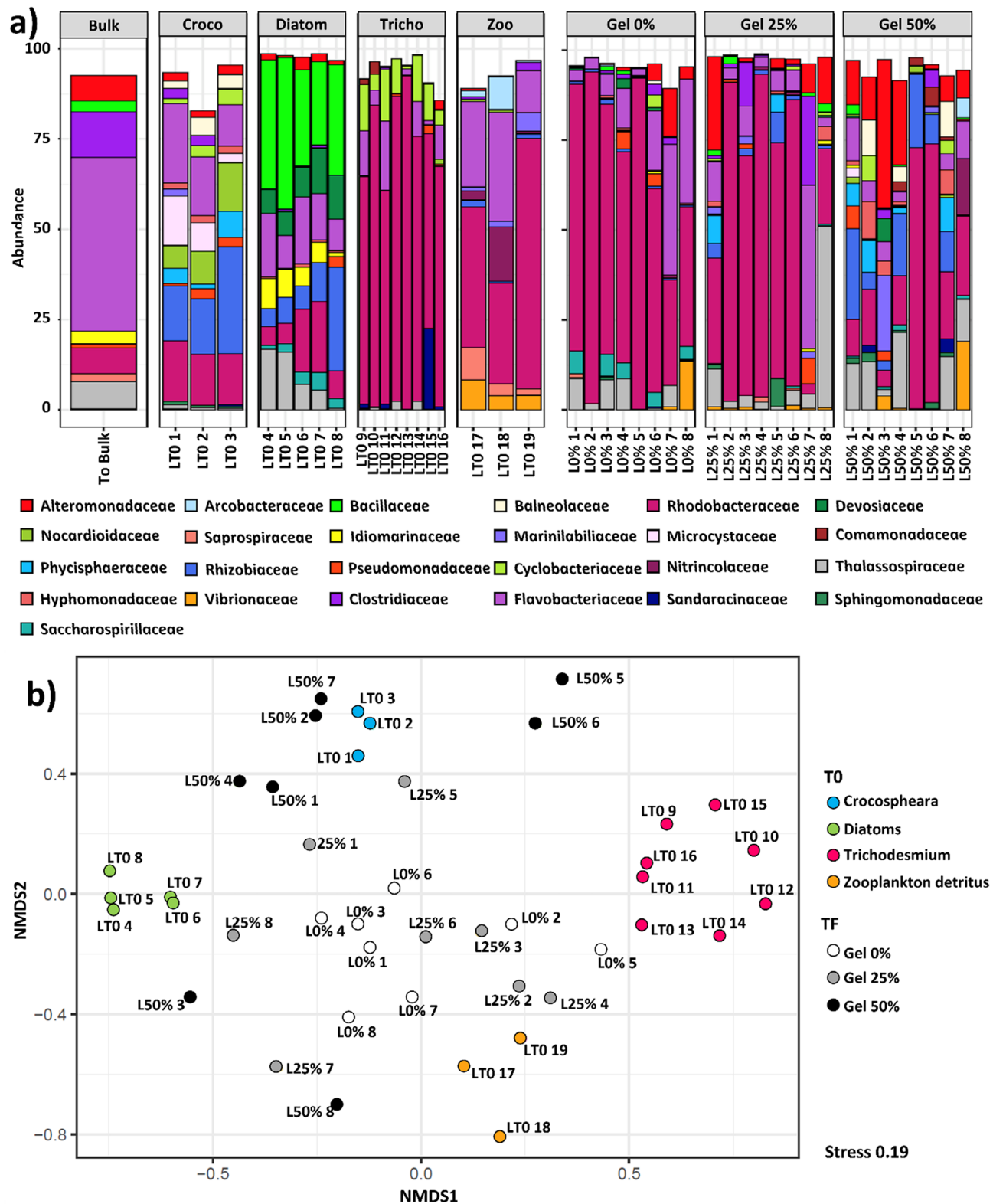


Fig. 2. Active bacterial community based on 16S rRNA before starting the experiment (T0), bulk samples, and individual particles, and after 4 d at in situ like conditions with three different gels containing either 0%, 25%, or 50% of RNA-fixative. **(a)** Bar plot of the relative abundance of the 25 most abundant families of active prokaryotes and **(b)** NMDS ordination plot (Bray–Curtis distance) showing the dissimilarity in active prokaryotes between individual particles. The stress value of the NMDS analysis is 0.19, which is closed but below the commonly accepted limit of 0.2 (Dexter et al. 2018).

were present in all particle types including Rhodobacteraceae and Flavobacteriaceae, yet with great variability in abundance between particle types (from 5% to 92% and from 0.17% to 30%, respectively). Nevertheless, 89% of all ASVs are present exclusively in one particle type and are absent from the other. For instance, the (i) Vibrionaceae (4–8%), Nitrospiraceae (0.6–15%), and Arcobacteraceae (0.4–9%) occurred exclusively on zooplankton detritus; (ii) Idiominaceae (2–8%), Devosiaceae (6.5–12.5%), and Bacillaceae (23–42%) on Diatoms particles; (iii) Sandaracinaceae (0.02–23%) on *Trichodesmium* particles; and (iv) Phycispheraceae (1.3–7.3%), Nocardiodaceae (6.2–13.4%), or Myrocystaceae (2.3–13.6%) on *Crocospaera* particles (Fig. 2). The T0 bulk sample did not represent the variability between particle types. Although 94% of all prokaryotic diversity of the bulk T0 corresponded to ASVs present in the individual particles, 16%, 19%, 14%, and 40% of the ASVs of *Crocospaera*, Diatoms, *Trichodesmium*, and zooplankton detritus, respectively, are absent from the T0 bulk sample. Consequently, in addition to not representing the total active prokaryotic diversity, the bulk approach does not distinguish between the type of particles.

Optimal RNA-fixative concentration in gels

To evaluate the effect of the jellified RNA-fixative on active particle attached bacterial communities, we tested three concentrations of RNA-fixative, that is, 0%, 25%, and 50% (called hereafter gel 0%, gel 25%, and gel 50%) after 4 d of incubation at in situ like conditions. Around 87% of the active prokaryotes found in the 50% gel, corresponded to ASVs also found in the individual particles at T0 (Fig. 2). The new incomers on the 50% gel accounted for 13% of the ASVs mostly with a sequence frequency below 0.1%. In contrast, new taxa found in the 0% and 25% gels reached similar proportion of total ASVs, but making up 2–13% or 3–21% (depending on the individual particle) of total diversity, respectively. Thus, 50% gels efficiently prevent the de novo colonization of particles by new communities while the particles are in the sediment trap.

The 25 most abundant active families recovered from individual particles in the three different gels are shown in Fig. 2. Only gel 50% allowed to derive from which type of T0 a particle originated. For instance, active bacteria of particle “L50% 8” are represented by 19% of Vibrionaceae, 16% of Nitrospiraceae and 5% of Arcobacteraceae, all three were present exclusively in zooplankton detritus particles at T0. Similarly, indicative patterns of *Crocospaera* particles in particle “L50% 1” can be seen for instance in the 3% of Myrocystaceae and 6% of Phycispheraceae which were both present exclusively in *Crocospaera* particles. As some particles aggregated while sinking, some particles may contain ASVs exclusive to different particle types at the same time. Gel 50% also allows best to reconstruct the mechanisms underlying this process. For particles recovered from gels 0% or 25% some taxa, mainly Rhodobacteraceae, dominated the prokaryotic diversity, sometimes up to 92% of the entire diversity. This is well confirmed by the non-metric multi-dimensional scaling (NMDS) (Fig. 2b) placing particles recovered from gels 0% and 25% in the

middle of the plot while gel 50% particles are well placed among the T0 particle types from which they were formed.

In situ deployment

Among all particles collected from the gel traps deployed during the EMSO-LO cruise, 10 particles from each gel (0% and 50%) were sampled for individual analysis of active microbial diversity. The individual particles were imaged (Fig. 3) and the 16S rRNA of the active bacterial community was subsequently sequenced. We identified four types of particles: fecal aggregates, single fecal pellets, phytodetrital aggregates and phytodetrital aggregates with fecal inclusions. The visual characterization of phytoplankton detritus was confirmed by the high percentage ($18\% \pm 9\%$) of sequences assigned to Chloroplast or to *Cyanobacteria* in the majority of particles of this type (Supporting Information Table S1). Particles were highly heterogenous in size ranging from 50 μm width and 300 μm length (“E50%2”) to 1880 width and 2880 μm length

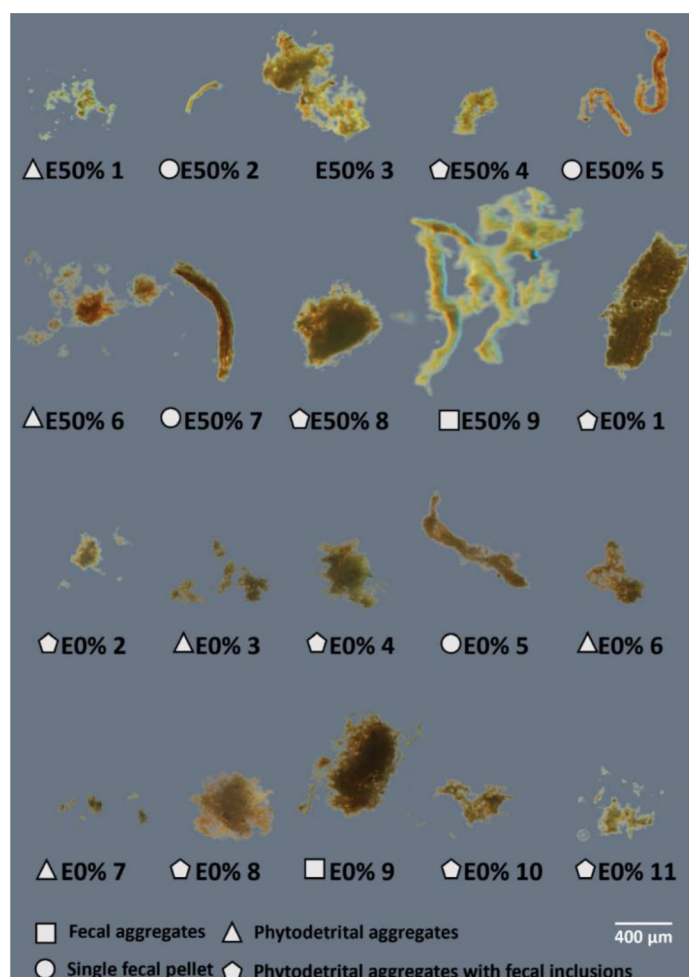


Fig. 3. Images of individual particles sampled in the RNA-fixative gel (at RNA-fixative concentrations of 0% and 50%) from a sediment trap deployed at 300 m during the EMSO-LO cruise ($42^{\circ}48.30\text{N}$, $0.5^{\circ}59.93\text{E}$, February 2022).

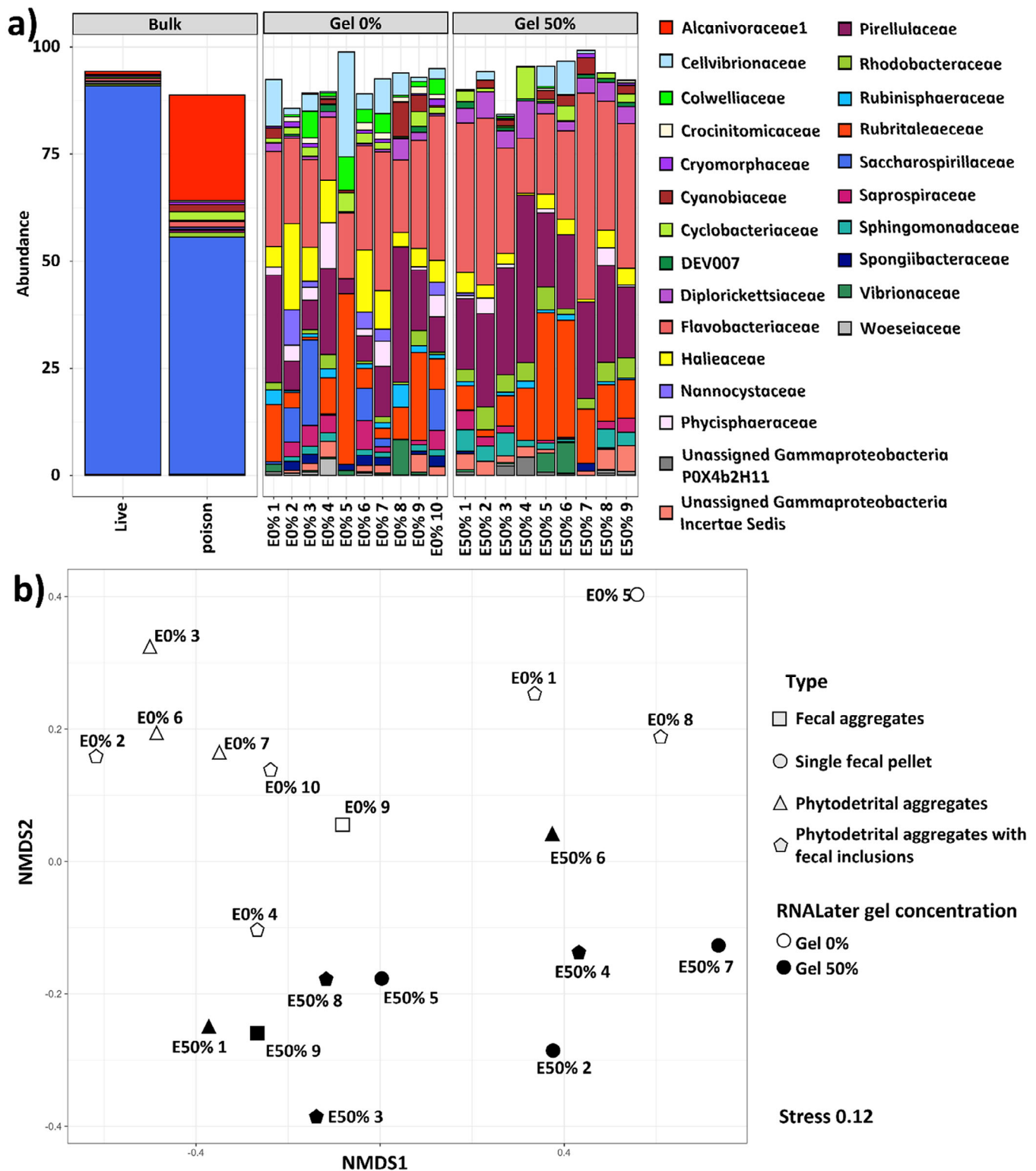


Fig. 4. Active bacterial diversity (16S rRNA metabarcoding) of individual particles recovered from RNA-fixative gels (with RNA fixative concentration of either 0% or 50%) during the EMSO-LO cruise (42°48.30N, 0.5°59.93E, February 2022). **(a)** Bar plot of the 25 most abundant families representing active prokaryotic diversity. Live bulk (0% RNA fixative) or poisoned (50% RNA fixative) are also shown for comparison. **(b)** NMDS ordination plot (Bray–Curtis distance) showing the dissimilarity of the active prokaryotes (at ASV level) between individual particles. The stress value of the NMDS analysis is 0.12, below the commonly accepted limit of 0.2 (Dexter et al. 2018).

(“E50%9”). Besides, we observed some unexpected characteristics such as “E0%9” representing a conglomerate of various fecal pellets (each $\approx 400 \mu\text{m}$ length) or “E0%11” which contains an intact organism.

This heterogeneity in particle type is also reflected in the diversity of the active microbial community (removing Chloroplasts for the analysis) associated with each individual particle. Regardless of the RNA-fixative concentration in the gels, richness varied from 59 to 250 ASVs without any distinct pattern with particle type or size. ASVs specific to one particle represent on average 65% of ASVs present on this same particle (19–45% depending on the individual particle). In addition, the bulk live revealed that 90% of the active bacterial diversity were just represented by two ASVs of Saccharospirillaceae (Fig. 4a). In the bulk poisoned, the active bacterial diversity is represented by the same two ASVs at 55%, plus one ASV of Alcanivoraceae at 24%. A presence absence analysis revealed that 76% and 75% of active prokaryotic ASVs from individual particles are absent in bulk live or poisoned, respectively. Consequently, as for the lab experiment, bulk samples do not reflect the active prokaryotic diversity and heterogeneity of individual particles (Fig. 4a).

NMDS analysis (Fig. 4b) does not reveal any clustering related to particle type or size. Although individual particles were separated on dimension 2 by RNA-fixative concentration in the gels (0% on the top and 50% near the bottom of the plot, ANOSIM test with Significance of 0.0168), our data do not provide any obvious reason to explain the separation in two groups by dimension 1 (right and left).

Discussion

Sediment traps collect mostly sinking particles that drive the gravitational POC export (McDonnell et al. 2015). This contrasts with sequential size-filtration of water samples which predominantly select suspended particles. By fitting specifically designed gels inside the tubes of drifting sediment traps, we were able to preserve the morphological structure of particles and at the same time to provide information on microbial diversity associated to individual particles in relation to their specific features (morphological). Without such gels, particles sink and accumulate at the bottom of the sediment traps where they lose their initial structure and thus the microbial communities associated to each single particle. In addition, the analysis of the mass accumulation of particles (so called “bulk approach”) requires filtration of the sediment trap material resulting in the destruction of individual particles and a complete loss of structural information. Comparing the results of lab experiments and field sampling, we demonstrate that the “bulk approach” is inadequate to resolve the true diversity of attached microbial communities as it yields to a prokaryotic diversity that is not representative of the sinking carbon flux (Figs. 2a, 4a). This is consistent with results from transparent exopolymer particles (Zäncker et al. 2019) and freshwater particles (Bižić-Ionescu et al. 2018). This can occur

due to the combination of two causes: (i) bulk approach mixes individual particles and thus masks the true heterogeneity of the sum of individual particles, and (ii) PCR artificially and exponentially amplifies the most abundant families in the bulk of particles, which does not necessarily account for those at the scale of individual particles. In other words, the most abundant families in the bulk are not necessarily the most abundant on each individual particle. This could be driven by a few heavily colonized larger particles that do not represent the majority of particles in the samples.

Effect of jellified RNA-fixative

By using different concentrations of RNA-fixative in bulk approaches and in gels (with or without in the bulk or 0%, 25%, and 50% in gels), we were able to assess the effects of RNA-fixative on the preservation of the natural diversity of active prokaryotes. During our 4-days long lab experiment, solely the 50% gel allowed to resolve the origin of individual particles as compared to gels with 0% and 25% RNA-fixative. Gels with low fixative concentrations (0 and 25%) did not fix the community efficiently and allowed prokaryotes to grow and dominate. This masked the true prokaryotic diversity of individual particles. For the field sediment trap deployment, we show differences between live and poisoned bulk samples, as well as clear differences in bacterial community composition between 0% and 50% gels (Fig. 4). Although the use of RNALater and similar fixatives is at times criticized for inducing biases in differential gene analysis (Passow et al. 2019), it has many advantages when it comes to inclusion in sediment traps. We therefore used RNALater-like fixation for its ability to fix the transcriptional image of the community until the sediment samples are collected and further processed. Drifting sediment trap arrays are often deployed for 4–6 d, a period which may alter natural microbial communities depending on the respective in situ conditions and particle concentration. Thus, our approach using jellified RNA-fixative avoids artificial shifts in microbial communities by efficiently preserving the RNA transcripts and the morphological characteristics of individual sinking particles. RNA degradation in RNALater-like fixatives was shown to occur after 8 months when stored at 5°C (Gorokhova 2005), yet our samples were stored at -80°C and were processed within 3 months from the cruise. Thus, neither the drifting time, nor our post-processing are likely to result in biases in the observed community and subsequently in future studies for meta-transcriptome analyses.

Toward prokaryotic diversity on individual sinking particles

Naturally formed marine particles are complex. Despite the clear identification of 4 distinct particle types (fecal aggregates, single fecal pellets, phytodetrital aggregates and phytodetrital aggregates with fecal inclusions) during the EMSO-LO cruise, such classification alone could not explain the observed differences in diversity between individual particles. No

relationship between particle size and active bacterial diversity was found either, even when richness (i.e., presence/absence) was considered. Looking at the processes responsible for heterogeneity during particles colonization is beyond the scope of this paper which focuses on the method to sample individual particles for downstream molecular analyses. However, we provide some possible explanations in the Supporting Information. In situ particles are naturally heterogeneous (Bizic-Ionescu et al. 2018; Zäncker et al. 2019; Szabo et al. 2022). Focusing our study on method development, the 10 particles analyzed do not show clear patterns here. However, by showing the ability to preserve the transcribed RNA and the associated microbial community, we open new horizons for future sea going campaigns. Particle composition and inherent physical, chemical, and morphological characteristics as well as stochastic processes or interactions between organisms drive prokaryotic diversity. In turn, diversity may drive associated remineralization rates (Munson-McGee et al. 2022). It seems thus essential to identify patterns between the types of individual particles that together form the gravitational flux and their associated microbial communities. Three decades ago, Fuhrman (1992) concluded that given the complexity of the oceanic microbial food web, it is not sufficient to solely consider parameters in bulk as the underlying mechanisms and processes can only be understood by examining the individual components. Nowadays, studies aiming to identify the ecological processes that structure microbial communities are often conducted by using observational data on species abundances (Armitage and Jones 2019). Yet, Armitage and Jones (2019) also conclude that this assumption is violated when a single sample unit contains processes of different scales. This is the case for a filter onto which hundreds or more of different sinking particles are collected, each potentially harboring different micro-niches harboring distinct attached prokaryotic communities. Armitage and Jones (2019) further conclude that measuring and accounting for heterogeneity at very small scales will lead to more reliable inferences of the ecological mechanisms structuring natural microbial communities. With no a priori information about particle sources, composition, and transformations that each sinking particle may have experienced, our experimental approach offers new horizons by enabling the understanding of phylogenetic and functional patterns and related physiological processes at the individual particle level. Given the wide range of potential particle origins and history, complementary analyses such as the 18S rRNA gene could provide more details on particle origin than optical images alone (Amacher et al. 2009; Duret et al. 2020; Durkin et al. 2022). Furthermore, simultaneous analyses of the 16S and 18S rRNA gene (or COI gene) could further reveal hidden links between origin and prokaryotic diversity of individual particles (Lundgreen et al. 2019).

Concluding remarks and further perspectives

Our method enables the collection of intact particles (in terms of structure and nucleic acid profiles) from any water

depth. We opened up the possibility to include microbial-scale processes in the equation with the goal to reliably define microbial functional groups and ultimately remineralization patterns at different spatial and temporal scales. RNA-fixative gels deployed at different depths will improve our understanding of the surface-depth connectivity in terms of microbial communities during particle degradation and changing environmental conditions (e.g., increasing pressure, changing temperature, O₂ concentration). Building such bridges between particle ecology (e.g., particle production, export, remineralization, sinking speed, etc.) and microbial ecology (microbial diversity, taxa co-occurrence, growth rates and activities) provide novel aspects to understand remineralization mechanisms and processes throughout the entire water column, different locations and seasons. The amount, timing and molecular composition of carbon uptake and release are still poorly understood mechanistically. Some models using genomic data (Saifuddin et al. 2019; Ofaim et al. 2021) or metagenomic data (Zorrilla et al. 2021) are emergent tools for probing the metabolic dynamics of microbial communities and link it to carbon utilization rates. Therefore, our RNA-fixative gels method also offers new perspectives improving available genomic and transcriptomic data obtained from individual particles to improve genome-scale metabolic models of particle-colonizing prokaryotes to more reliably predict carbon fluxes.

References

- Allredge, A. L., and M. W. Silver. 1988. Characteristics, dynamics and significance of marine snow. *Prog. Oceanogr.* **20**: 41–82. doi:10.1016/0079-6611(88)90053-5
- Amacher, J., S. Neuer, I. Anderson, and R. Massana. 2009. Molecular approach to determine contributions of the protist community to particle flux. *Deep Sea Res. I Oceanogr. Res. Pap.* **56**: 2206–2215. doi:10.1016/j.dsr.2009.08.007
- Armitage, D. W., and S. E. Jones. 2019. How sample heterogeneity can obscure the signal of microbial interactions. *ISME J.* **13**: 2639–2646. doi:10.1038/s41396-019-0463-3
- Armstrong, R. A., C. Lee, J. I. Hedges, S. Honjo, and S. G. Wakeham. 2002. A new, mechanistic model for organic carbon fluxes in the ocean based on the quantitative association of POC with ballast minerals. *Deep Sea Res. II Top. Stud. Oceanogr.* **49**: 219–236. doi:10.1016/S0967-0645(01)00101-1
- Baumas, C. M. J., and others. 2021. Mesopelagic microbial carbon production correlates with diversity across different marine particle fractions. *ISME J.* **15**: 1695–1708. doi:10.1038/s41396-020-00880-z
- Baumas, C. M. J., and M. Bizic. 2023. Did you say marine snow? Zooming into different types of organic matter particles and their importance in the open ocean carbon cycle. doi:10.31223/X5RM1T
- Belcher, A., M. Iversen, S. Giering, V. Riou, S. A. Henson, L. Berline, L. Guilloux, and R. Sanders. 2016. Depth-resolved

- particle-associated microbial respiration in the northeast Atlantic. *Biogeosciences* **13**: 4927–4943. doi:10.5194/bg-13-4927-2016
- Bizic, M., and others. 2022. Land-use type temporarily affects active pond community structure but not gene expression patterns. *Mol. Ecol.* **31**: 1716–1734. doi:10.1111/mec.16348
- Bizic-Ionescu, M., D. Ionescu, and H.-P. Grossart. 2018. Organic particles: Heterogeneous hubs for microbial interactions in aquatic ecosystems. *Front. Microbiol.* **9**: 1–15. doi:10.3389/fmicb.2018.02569
- Callahan, B. J., P. J. McMurdie, M. J. Rosen, A. W. Han, A. J. A. Johnson, and S. P. Holmes. 2016. DADA2: High-resolution sample inference from Illumina amplicon data. *Nat. Methods* **13**: 581–583. doi:10.1038/nmeth.3869
- Chen, Y.-B., J. P. Zehr, and M. Mellon. 1996. Growth and nitrogen fixation of the diazotrophic filamentous nonheterocystous cyanobacterium *Trichodesmium* sp. IMS 101 in defined media: Evidence for a circadian rhythm. *J. Phycol.* **32**: 916–923. doi:10.1111/j.0022-3646.1996.00916.x
- Choi, Y., A. Kim, J. Kim, J. Lee, S. Y. Lee, and C. Kim. 2017. Optimization of RNA extraction from formalin-fixed paraffin-embedded blocks for targeted next-generation sequencing. *J. Breast Cancer* **20**: 393–399. doi:10.4048/jbc.2017.20.4.393
- Cordero, O. X., and M. S. Datta. 2016. Microbial interactions and community assembly at microscales. *Curr. Opin. Microbiol.* **31**: 227–234. doi:10.1016/j.mib.2016.03.015
- De Giorgi, C., M. Finetti Sialer, and F. Lamberti. 1994. Formalin-induced infidelity in PCR-amplified DNA fragments. *Mol. Cell. Probes* **8**: 459–462. doi:10.1006/mcpr.1994.1065
- Dexter, E., G. Rollwagen-Bollens, and S. M. Bollens. 2018. The trouble with stress: A flexible method for the evaluation of nonmetric multidimensional scaling. *Limnol. Oceanogr. Methods* **16**: 434–443. doi:10.1002/lom3.10257
- Doolittle, W. F., and O. Zhaxybayeva. 2013. What is a prokaryote? p. 21–37. *In* E. Rosenberg, E. F. DeLong, S. Lory, E. Stackebrandt, and F. Thompson [eds.], *The prokaryotes: Prokaryotic biology and symbiotic associations*. Springer.
- Duret, M. T., R. S. Lampitt, and P. Lam. 2019. Prokaryotic niche partitioning between suspended and sinking marine particles. *Environ. Microbiol. Rep.* **11**: 386–400. doi:10.1111/1758-2229.12692
- Duret, M. T., R. S. Lampitt, and P. Lam. 2020. Eukaryotic influence on the oceanic biological carbon pump in the Scotia Sea as revealed by 18S rRNA gene sequencing of suspended and sinking particles. *Limnol. Oceanogr.* **65**: S49–S70. doi:10.1002/lno.11319
- Durkin, C. A., I. Cetinić, M. Estapa, Z. Ljubešić, M. Mucko, A. Neeley, and M. Omand. 2022. Tracing the path of carbon export in the ocean through DNA sequencing of individual sinking particles. *ISME J.* **16**: 1–11. doi:10.1038/s41396-022-01239-2
- Evers, D. L., C. B. Fowler, B. R. Cunningham, J. T. Mason, and T. J. O’Leary. 2011. The effect of formaldehyde fixation on RNA. *J. Mol. Diagn.* **13**: 282–288. doi:10.1016/j.jmoldx.2011.01.010
- Fontanez, K. M., J. M. Eppley, T. J. Samo, D. M. Karl, and E. F. DeLong. 2015. Microbial community structure and function on sinking particles in the North Pacific subtropical gyre. *Front. Microbiol.* **6**: 1–14. doi:10.3389/fmicb.2015.00469
- Frank, A. H., J. A. L. Garcia, G. J. Herndl, and T. Reinthaler. 2016. Connectivity between surface and deep waters determines prokaryotic diversity in the North Atlantic deep water. *Environ. Microbiol.* **18**: 2052–2063. doi:10.1111/1462-2920.13237
- Fuchs, R., C. M. J. Baumas, M. Garel, D. Nerini, F. A. C. Le Moigne, and C. Tamburini. 2022. A RUpture-based detection method for the active mesopelagic zone (RUBALIZ): A crucial step toward rigorous carbon budget assessments. *Limnol. Oceanogr. Methods* **21**: 24–39. doi:10.1002/lom3.10520
- Fuhrman, J. 1992. Bacterioplankton roles in cycling of organic matter: the microbial food web, p. 361–383. *In* Primary productivity and biogeochemical cycles in the sea. Springer.
- Ganesh, S., D. J. Parris, E. F. DeLong, and F. J. Stewart. 2014. Metagenomic analysis of size-fractionated picoplankton in a marine oxygen minimum zone. *ISME J.* **8**: 187–211. doi:10.1038/ismej.2013.144
- Gorokhova, E. 2005. Effects of preservation and storage of microcrustaceans in RNA later on RNA and DNA degradation. *Limnol. Oceanogr. Methods* **3**: 143–148. doi:10.4319/lom.2005.3.143
- Gray, M. A., Z. A. Pratte, and C. A. Kellogg. 2013. Comparison of DNA preservation methods for environmental bacterial community samples. *FEMS Microbiol. Ecol.* **83**: 468–477. doi:10.1111/1574-6941.12008
- Grossart, H. P., T. Kjørboe, K. W. Tang, M. Allgaier, E. M. Yam, and H. Ploug. 2006. Interactions between marine snow and heterotrophic bacteria: Aggregate formation and microbial dynamics. *Aquat. Microb. Ecol.* **42**: 19–26. doi:10.3354/ame042019
- Guidi, L., G. A. Jackson, L. Stemann, J. C. Miquel, M. Picheral, and G. Gorsky. 2008. Relationship between particle size distribution and flux in the mesopelagic zone. *Deep Sea Res. I Oceanogr. Res. Pap.* **55**: 1364–1374. doi:10.1016/j.dsr.2008.05.014
- Guillard, R. R. L. 1975. Culture of phytoplankton for feeding marine invertebrates, p. 29–60. *In* W. L. Smith and M. H. Chanley [eds.], *Culture of marine invertebrate animals: Proceedings—1st conference on Culture of marine invertebrate animals Greenport*. Springer.
- Guillard, R. R. L., and P. E. Hargraves. 1993. *Stichochrysis immobilis* is a diatom, not a chrysophyte. *Phycologia* **32**: 234–236. doi:10.2216/i0031-8884-32-3-234.1
- Henson, S. A., R. Sanders, E. Madsen, P. J. Morris, F. Le Moigne, and G. D. Quartly. 2011. A reduced estimate of the strength of the ocean’s biological carbon pump. *Geophys. Res. Lett.* **38**: 1–5. doi:10.1029/2011GL046735

- Hykin, S. M., K. Bi, and J. A. McGuire. 2015. Fixing formalin: A method to recover genomic-scale DNA sequence data from formalin-fixed museum specimens using high-throughput sequencing. *PLoS One* **10**: e0141579. doi:10.1371/journal.pone.0141579
- Kjørboe, T., and G. A. Jackson. 2001. Marine snow, organic solute plumes, and optimal chemosensory behavior of bacteria. *Limnol. Oceanogr.* **46**: 1309–1318. doi:10.4319/lo.2001.46.6.1309
- Klindworth, A., E. Pruesse, T. Schweer, J. Peplies, C. Quast, M. Horn, and F. O. Glöckner. 2013. Evaluation of general 16S ribosomal RNA gene PCR primers for classical and next-generation sequencing-based diversity studies. *Nucleic Acids Res.* **41**: e1. doi:10.1093/nar/gks808
- Kwon, E. Y., F. Primeau, and J. L. Sarmiento. 2009. The impact of remineralization depth on the air–sea carbon balance. *Nat. Geosci.* **2**: 630–635. doi:10.1038/ngeo612
- Lane, D. J. 1991. 16S/23S rRNA sequencing. *In* *Nucleic Acid Techniques in Bacterial Systematics*. Wiley.
- Laurenceau-Cornec, E. C., F. A. C. Le Moigne, M. Gallinari, B. Moriceau, J. Toullec, M. H. Iversen, A. Engel, and C. L. De La Rocha. 2019. New guidelines for the application of Stokes' models to the sinking velocity of marine aggregates. *Limnol. Oceanogr.* **1–22**: 1264–1285. doi:10.1002/lno.11388
- Le Moigne, F. A. C. 2019. Pathways of organic carbon downward transport by the oceanic biological carbon pump. *Front. Mar. Sci.* **6**: 1–8. doi:10.3389/fmars.2019.00634
- Lundgreen, R. B. C., C. Jaspers, S. J. Traving, and others. 2019. Eukaryotic and cyanobacterial communities associated with marine snow particles in the oligotrophic Sargasso Sea. *Sci. Rep.* **9**: 8891. doi:10.1038/s41598-019-45146-7
- Martin, J. H., G. A. Knauer, D. M. Karl, and W. W. Broenkow. 1987. VERTEX: Carbon cycling in the northeast Pacific. *Deep Sea Res. A Oceanogr. Res. Pap.* **34**: 267–285. doi:10.1016/0198-0149(87)90086-0
- McDonnell, A. M. P., and others. 2015. The oceanographic toolbox for the collection of sinking and suspended marine particles. *Prog. Oceanogr.* **133**: 17–31. doi:10.1016/j.pocean.2015.01.007
- Mestre, M., C. Ruiz-González, R. Logares, C. M. Duarte, J. M. Gasol, and M. M. Sala. 2018. Sinking particles promote vertical connectivity in the ocean microbiome. *Proc. Natl. Acad. Sci. USA* **115**: E6799–E6807. doi:10.1073/pnas.1802470115
- Munson-McGee, J. H., and others. 2022. Decoupling of respiration rates and abundance in marine prokaryoplankton. *Nature* **612**: 1–7. doi:10.1038/s41586-022-05505-3
- Ofaim, S., S. Sulheim, E. Almaas, D. Sher, and D. Segrè. 2021. Dynamic allocation of carbon storage and nutrient-dependent exudation in a revised genome-scale model of *Prochlorococcus*. *Front. Genet.* **12**: 1–12. doi:10.3389/fgene.2021.586293
- Oksanen, J., and others. 2020. vegan: Community ecology package. doi:10.3389/fpsyg.2020.568256
- Pace, N. R. 2006. Time for a change. *Nature* **441**: 289. doi:10.1038/441289a
- Paliy, O., H. Kenche, F. Abernathy, and S. Michail. 2009. High-throughput quantitative analysis of the human intestinal microbiota with a phylogenetic microarray. *Appl. Environ. Microbiol.* **75**: 3572–3579. doi:10.1128/AEM.02764-08
- Passow, C. N., T. J. Y. Kono, B. A. Stahl, J. B. Jaggard, A. C. Keene, and S. E. McGaugh. 2019. Nonrandom RNAseq gene expression associated with RNAlater and flash freezing storage methods. *Mol. Ecol. Resour.* **19**: 456–464. doi:10.1111/1755-0998.12965
- Pelve, E. A., K. M. Fontanez, and E. F. DeLong. 2017. Bacterial succession on sinking particles in the ocean's interior. *Front. Microbiol.* **8**: 1–15. doi:10.3389/fmicb.2017.02269
- Planquette, H., and R. M. Sherrell. 2012. Sampling for particulate trace element determination using water sampling bottles: Methodology and comparison to in situ pumps. *Limnol. Oceanogr. Methods* **10**: 367–388. doi:10.4319/lom.2012.10.367
- Ploug, H., and H. Grossart. 1999. Bacterial production and respiration in suspended aggregates—A matter of the incubation method. *Aquat. Microb. Ecol.* **20**: 21–29. doi:10.3354/ame020021
- Puigcorbè, V., C. Ruiz-González, P. Masqué, and J. M. Gasol. 2020. Sampling device-dependence of prokaryotic community structure on marine particles: Higher diversity recovered by in situ pumps than by oceanographic bottles. *Front. Microbiol.* **11**: 1645. doi:10.3389/fmicb.2020.01645
- Quast, C., E. Pruesse, P. Yilmaz, J. Gerken, T. Schweer, P. Yarza, J. Peplies, and F. O. Glöckner. 2013. The SILVA ribosomal RNA gene database project: Improved data processing and web-based tools. *Nucleic Acids Res.* **41**: D590–D596. doi:10.1093/nar/gks1219
- Saifuddin, M., J. M. Bhatnagar, D. Segrè, and A. C. Finzi. 2019. Microbial carbon use efficiency predicted from genome-scale metabolic models. *Nat. Commun.* **10**: 3568. doi:10.1038/s41467-019-11488-z
- Salazar, G., F. M. Cornejo-Castillo, V. Benítez-Barrios, E. Fraile-Nuez, X. A. Álvarez-Salgado, C. M. Duarte, J. M. Gasol, and S. G. Acinas. 2016. Global diversity and biogeography of deep-sea pelagic prokaryotes. *ISME J.* **10**: 596–608. doi:10.1038/ismej.2015.137
- Siegel, D. A., and others. 2016. Prediction of the export and fate of global ocean net primary production: The EXPORTS science plan. *Front. Mar. Sci.* **3**: 22. doi:10.3389/fmars.2016.00022
- Siegel, D. A., T. DeVries, I. Cetinić, and K. M. Bisson. 2023. Quantifying the ocean's biological pump and its carbon cycle impacts on global scales. *Annu. Rev. Mar. Sci.* **15**: 329–356. doi:10.1146/annurev-marine-040722-115226
- Simon, M., H. Grossart, B. Schweitzer, and H. Ploug. 2002. Microbial ecology of organic aggregates in aquatic

- ecosystems. *Aquat. Microb. Ecol.* **28**: 175–211. doi:[10.3354/ame028175](https://doi.org/10.3354/ame028175)
- Smith, D. C., M. Simon, A. L. Alldredge, and F. Azam. 1992. Intense hydrolytic enzyme activity on marine aggregates and implications for rapid particle dissolution. *Nature* **359**: 139–142. doi:[10.1038/359139a0](https://doi.org/10.1038/359139a0)
- Stief, P., M. Elvert, and R. N. Glud. 2021. Respiration by “marine snow” at high hydrostatic pressure: Insights from continuous oxygen measurements in a rotating pressure tank. *Limnol. Oceanogr.* **66**: 2797–2809. doi:[10.1002/lno.11791](https://doi.org/10.1002/lno.11791)
- Szabo, R. E., S. Pontrelli, J. Grilli, J. A. Schwartzman, S. Pollak, U. Sauer, and O. X. Cordero. 2022. Historical contingencies and phage induction diversify bacterioplankton communities at the microscale. *Proc. Natl. Acad. Sci. USA* **119**: e2117748119. doi:[10.1073/pnas.2117748119](https://doi.org/10.1073/pnas.2117748119)
- Thiele, S., B. M. Fuchs, R. Amann, and M. H. Iversen. 2015. Colonization in the photic zone and subsequent changes during sinking determine bacterial community composition in marine snow. *Appl. Environ. Microbiol.* **81**: 1463–1471. doi:[10.1128/AEM.02570-14](https://doi.org/10.1128/AEM.02570-14)
- Trull, T. W., S. G. Bray, K. O. Buesseler, C. H. Lamborg, S. Manganini, C. Moy, and J. Valdes. 2008. In situ measurement of mesopelagic particle sinking rates and the control of carbon transfer to the ocean interior during the vertical flux in the Global Ocean (VERTIGO) voyages in the North Pacific. *Deep Sea Res. II Top. Stud. Oceanogr.* **55**: 1684–1695. doi:[10.1016/j.dsr2.2008.04.021](https://doi.org/10.1016/j.dsr2.2008.04.021)
- Turner, J. T. 2015. Zooplankton fecal pellets, marine snow, phytodetritus and the ocean’s biological pump. *Prog. Oceanogr.* **130**: 205–248. doi:[10.1016/j.pocean.2014.08.005](https://doi.org/10.1016/j.pocean.2014.08.005)
- Zäncker, B., A. Engel, and M. Cunliffe. 2019. Bacterial communities associated with individual transparent exopolymer particles (TEP). *J. Plankton Res.* **41**: 561–565. doi:[10.1093/plankt/fbz022](https://doi.org/10.1093/plankt/fbz022)
- Zorrilla, F., F. Buric, K. R. Patil, and A. Zelezniak. 2021. metaGEM: Reconstruction of genome scale metabolic models directly from metagenomes. *Nucleic Acids Res.* **49**: e126. doi:[10.1093/nar/gkab815](https://doi.org/10.1093/nar/gkab815)

Acknowledgments

We thank the crew and officers of the N/O Le Pourquoi Pas? (Flotte Océanographique Française) for their professional help during the EMSO-LO cruise (Chief scientist Dominique Lefèvre). This work benefited from services provided by the EMSO_ERIC Virtual Organization, supported by the national resource providers of the EGI Federation (EMSO-France CNRS-IFREMER) for sustainability of the moored research infrastructure. Part of the equipment used in this work was funded by the European Regional Development Fund (ERDF). The authors also thank the OMICS, SAM, PACEM, and CULTURE—MIO platforms for sample analyses. We thank Vincent Garel for the cropping and assembling of the pictures of particles (Fig. 3) and Fabrizio D’Ortenzio for Chlorophyll data. This work was partly supported by the French National program LEFE (Les Enveloppes Fluides et l’Environnement, INSU—CNRS), through the PARTY project (remineralization des PARTICULES marines et Transfert vers les abYsses) awarded to FACLM and from own resources (PROTISVALOR) allocated to C.T. This manuscript is a contribution of the ANR APERO (project number ANR-21-CE01-0027). H.P.G. was supported by the Zooflux and Pycnotrap projects (GR1540/19-1 and GR1540/37-1) of the German Science Foundation (DFG).

Submitted 14 March 2023

Revised 25 August 2023

Accepted 20 October 2023

Associate editor: Gordon T. Taylor